Coronary Artery Spasm Related to Thiol Oxidation and Senescence Marker Protein-30 in Aging

Brief title: SMP30 and coronary artery spasm

Shinya Yamada,[1] Shu-ichi Saitoh,[1] Hirofumi Machii,[1] Hiroyuki Mizukami,[1] Yasuto Hoshino,[1] Tomofumi Misaka,[1] Akihito Ishigami,[2] Yasuchika Takeishi[1]

From the Department of Cardiology and Hematology, Fukushima Medical University, 1 Hikarigaoka, Fukushima, Japan (S. Y., S. S., H. Machii, H. Mizukami, T. M., Y. T.);

Molecular Regulation of Aging, Tokyo Metropolitan Institute of Gerontology, 35-2 Sakae-cho, Itabashi-ku, Tokyo, Japan (A.I.).

Department of Cardiology and Hematology
Fukushima Medical University, 1 Hikarigaoka, Fukushima 960-1295, Japan.

Abstract

Background: Senescence marker protein-30 (SMP30) decreases with aging, and SMP30 knock-out (KO) mice show a short life with increased oxidant stress. ***Aims:*** We assessed the effect of oxidant stress with SMP30 deficiency in coronary artery spasm and clarify its underlying mechanisms. ***Results***: We measured vascular responses to acetylcholine (ACh) and sodium nitroprusside (SNP) of isolated coronary arteries from SMP30 KO and wild-type (WT) mice. In SMP30 KO mice, ACh-induced vasoconstriction occurred, which was changed to vasodilation by dithiothreitol, a thiol-reducing agent (DTT). However, L-NAME, nitric oxide synthase inhibitor or tetrahydrobiopterin did not change the ACh response. In isolated coronary arteries of WT mice, ACh-induced vasodilation occurred. Inhibition of glutathione reductase by 1, 3-bis (2-chloroethyl)-1-nitrosourea decreased ACh-induced vasodilation (n=10, P<0.01), which was restored by DTT. To evaluate the thiol oxidation, we measured the fluorescence of monochlorobimane (MCB) in coronary arteries, which covalently labels the total. The fluorescence level to MCB decreased in SMP30 KO mice, but with DTT treatment restored to a level comparable to that of WT mice. The reduced glutathione and total thiols level were also low in the aorta of SMP30 KO mice compared with those of WT mice. Administration of ACh into the aortic sinus *in vivo* of SMP30

KO mice induced coronary artery spasm. ***Innovation:*** The thiol redox state is a key regulator of eNOS activity, and thiol-oxidation was associated with endothelial dysfunction in the SMP30 deficiency model. ***Conclusion***: These results suggest that chronic thiol oxidation by oxidant stress is a trigger of coronary artery spasm, resulting in impaired endothelium-dependent vasodilation.

Innovation

Age-related oxidant stress with decrease of senescence marker protein-30 (SMP30) plays a pivotal role in coronary artery spasm, which is a major health problem. Nitric oxide generation in eNOS is of critical importance in maintaining proper coronary circulation. Chronic oxidant stress, through NADPH oxidase activation with the SMP30 deficiency, induced thiol oxidation in endothelial nitric oxide synthase (eNOS), and attenuated bioactive nitric oxide generation resulted in coronary artery spasm. The specifying of thiol redox state as a key regulator of eNOS activity provides a new platform for strategies to prevent coronary artery spasm and alleviate the underlying process of aging-induced coronary artery disease.

Key Words

SMP30

coronary artery spasm

oxidant stress

thiol oxidation

Abbreviations Used

ACh = acetylcholine

ADMA = asymmetric dimethylarginine

BCNU = 1, 3-bis (2-chloroethyl)-1-nitrosourea

BH_4 = tetrahydrobiopterin

DCF = dichlorodihydro-fluorescein fluorescence

DHE = dihydroethidium

DTT = dithiothreitol

eNOS = endothelial nitric oxide synthase

GSH = reduced glutathione

GSSG = oxidized glutathione

H_2O_2 = hydrogen peroxide

KO = knock out

L-NAME = N^{ω}-nitro-L-arginine-methyl ester

MBB = monobromotrimethylammoniobimane

MCB = monochlorobimane

NO = nitric oxide

ROS = reactive oxygen species (ROS)

SMP30 = senescence marker protein-30

SNP = sodium nitroprusside

WT = wild type

Introduction

Coronary artery spasm plays an important role in ischemic heart conditions especially in Japan, in forms such as variant angina (35). It has become a clinical problem in the Western world, leading to a rise in complex and aggressive of coronary interventions (25, 30). Recent advances in research on the pathogenesis of coronary artery spasms indicate the presence of endothelial dysfunction, which may be mediated by impaired endothelial nitric oxide synthase (eNOS) activity or primarily smooth muscle cell contraction with Rho-kinase activation in the spasm site (21, 28, 38). Also, aging associated with oxidant stress elevation is an important risk factor for development of ischemic heart disease (10). In the clinical setting, a shift in the redox equilibrium to a more oxidative state reportedly exists in patients with coronary artery spasm (27). However, the underlying mechanism of coronary artery spasm and age-related oxidant stress remains elusive.

The oxidation of the thiol group, including cysteine, is involved in many biological processes. Thiol oxidation induces protein conformation changes by converting free thiols (-SH) into sulfenic acids (SO-), sulfinic acids (SOO-), sulfonic acids (SOOO-), and disulfide bridges (S-S) (34). Thiol oxidation is involved in many cellular processes, such as eNOS glutathionylation (6), increased ryanodine receptor activity, inhibition of SERCA activity (46), and pulmonary artery vasoconstriction (26). Recently,

we observed that reactive oxygen species regulate coronary vascular tone mediated by thiol oxidation (33). Thus, we hypothesized that thiol oxidation with chronic oxidant stress plays a key role in age-related coronary artery spasm. Senescence marker protein-30 (SMP30), a 34-kDa protein originally identified in the rat liver, is an age-associated protein, and its production decreases with aging in the liver, kidneys, and lungs (48). SMP30 knock-out (KO) mice cannot synthesize vitamin C *in vivo* and have a short life. Humans are similarly incapable of synthesizing vitamin C. With aging, SMP30 content decreases in the liver, kidney, and lung in human, and such a SMP30 deficiency increases superoxide production (19, 20). Therefore, SMP30 KO mouse is a suitable model to test this hypothesis. Then we determined the role of oxidative stress related to thiol-oxidation in the redox dependent regulation of coronary vascular tone associated with nitric oxide (NO) generation, including coronary vasospasm using SMP30 KO mice coronary arteries.

Materials and Methods

Animal condition

SMP30 KO mice were bred from C57BL/6 mice by a gene targeting technique, as described previously (17). WT C57BL/6 and SMP30 KO mice (age 8-10 W, B.W., 22.5±2.6 g) were housed and bred in a room at 22±3°C, with a relative humidity of 50±10% and a 12-hour light-dark cycle. They were given food including vitamin C 21 mg/100 g (CLEA Japan, Tokyo, Japan) and water *ad libitum*. This investigation conformed to the Guideline on Animal Experiments of Fukushima Medical University, the Japanese Government Animal Protection and Management Law (No. 105), and the Guide for the Care and Use of Laboratory Animals (NIH Publication No. 85-23, revised 1996).

All reagents were obtained from Sigma-Aldrich (St. Louis, USA).

Measurements of nitric oxide and vitamin C level

After the mice were anesthetized by an intraperitoneal injection of sodium pentobarbital (50 mg/kg) and mid-sternotomies were performed, the aortas were isolated. In the aortas of SMP30 KO mice (n=10, 45.5±7.8 mg) and WT mice (n=10, 49.3±5.8 mg), NO concentrations induced by ACh were measured by a free radical analyzer (Apollo 4000, WPI Co., Ltd., FL) (32). Vitamin C in the aortas was measured by a high-performance

liquid chromatography with electrochemical detection method (18).

Experimental procedures

The mice were heparinized (400 units/kg i.p.) and anesthetized with sodium pentobarbital (50 mg/kg, i.p.). The hearts were removed and placed in buffered physiological salt solution (PSS) to pH 7.4 at 4°C, and prepared for vessel dissection. The bathing solution used for vessel dissection had the following composition (in mmol/l): NaCl 145.0, KCl 4.7, $CaCl_2$ 2.0, $MgSO_4$ 1.17, NaH_2PO_4 1.2, glucose 5.0, pyruvate 2.0, EDTA 0.02, 3-*N*-morpholino propanesulfonic acid buffer (MOPS) 3.0, and 1% bovine serum albumin (1 g/100 ml).

Left anterior descending arteries or circumflex coronary arteries from the left ventricle [84±8 (70-112) μm in diameter] were isolated under microscope (24, 33, 34). Each artery with its surrounding ventricular muscle was excised, transferred to a temperature-controlled dissection dish (4°C) containing PSS, and dissected free of muscle tissue. The side branches were tied off using an 11-0 suture. The vessels were transferred to a lucite chamber and cannulated at both ends using micropipettes and pressurized at 60 mmHg. Arteries were tied to each pipette using an 11-0 suture. The PSS, bubbled with 20% O_2, 5% CO_2, and 75% N_2, used to perfuse the vessels during the experiments was buffered to pH 7.4 at 37°C. The preparation was then transferred to the stage of an inverted microscope.

To assess leaks, the pressure at zero flow was measured, which should be equal to that of the inflow reservoir pressure when there are no leaks. Any preparations showing leaks were discarded. The vessels were slowly warmed to 37°C and allowed to develop a spontaneous tone.

Measurement of vessel diameter

First, the control inner diameter of the isolated coronary artery from the SMP30 KO and WT mice was measured at 37°C in a vessel chamber (2 ml) with an Olympus IX71 inverted microscope. In the SMP30 KO mice, vasodilative responses to increasing concentrations of ACh with or without DTT, L-NAME and BH_4, were measured. In the WT mice, vasodilative responses to increasing concentrations of ACh with or without BCNU, DTT or L-NAME, were measured. In the SMP30 KO and WT mice, vasodilative responses to increasing concentrations of SNP were measured.

Amplex-red assay for hydrogen peroxide production.

Freshly isolated aortic rings (4 × 2 mm) were used for assessment of H_2O_2 production using a fluorometric horseradish peroxidase assay (Amplex-Red assay, Molecular Probes, Eugene, Oregon). Fluorescence was measured (excitation 530 nm and emission 590 nm) after 1 h of incubation at 37°C in the dark against background fluorescence of buffer. Polyethylene glycol–conjugated catalase (300 units/ml; Sigma) inhibitable fraction

reflects specific H_2O_2 signal. The rate of H_2O_2 production was presented as picomoles per milligram protein per minute after calculation, according to a standard curve generated using fresh hydrogen peroxide in reaction buffer (5).

Asymmetric dimethylarginine concentration

Plasma and tissue ADMA concentration was determined by using a commercially available enzyme-linked immunosorbent assay kit (DLD Diagnostika GmbH, Hamburg, Germany) according to the manufacturer's instructions (23).

Tissue glutathione and total thiol concentrations in aorta

Total thiols were determined in aorta homogenates by measuring the absorbance of 5-thio-2-nitrobenzoic acid, the reaction product of sulfhydryl groups with 5, 5'-dithiobis-2-nitrobenzoic acid (Ellman's reagent). An equal volume of 10% metaphosphoric acid was added to the samples, the resulting precipitated proteins were pelleted by centrifugation, and the supernatant was neutralized with 50 µL/mL of 4 mol/L triethanolamine. Thiols were then measured by adding 200 µL Ellman's reagent from a commercially available assay to 50 µL of neutralized supernatant. The absorbance of the Ellman's reagent adduct was measured at 405 nm (39). Tissue concentrations of glutathione (total, reduced, and oxidized) were

measured in tissue homogenates (10% wt/vol) after deproteinization with metaphosphoric acid in an enzymatic recycling method with glutathione reductase as provided by a commercially available assay (Cayman Chemical Co., Michigan) (1). Values were normalized to protein concentration in the homogenate.

Measurement of fluorescence

The isolated arteries were placed on a slideglass and incubated for 5-min at 37°C with DHE or DCF. To assess the distribution of DHE or DCF, arteries were scanned by an Olympus IX71 inverted microscope (Olympus CCD, Tokyo, Japan). DHE or DCF staining was also performed with apocynin (20 min). MCB or MBB was administered to the isolated coronary arteries without any treatment, or after the administration of ACh or DTT in the conditioned buffer (5 min). The vessels were exposed to the fluorochromes for 30 min. Fluorescence was measured using fluorescein isothiocyanate excitation/emission spectra from digitized images, and normalized to the vessel area (expressed as intensity/100 μm^2). All camera settings were maintained constant throughout the image analyses (33). We measured the fluorescence intensities of 5 isolated coronary arteries in each heart, and averaged the data (43).

Measurement of ST-T segment changes in electrocardiogram

After the mice were anesthetized with an intraperitoneal injection of 2, 2, 2- tribromoethanol (250 mg/kg), ACh was administered by inserting a 27-G catheter from the cervical artery to the aortic sinus in the SMP30 KO and WT mice. The standard limb leads, aV_R, aV_L, and aV_F of the electrocardiogram were recorded by an electrocardiograph during 1-min intervals, and were constantly monitored (ECG-9122, Nihon Kohden, Tokyo, Japan). Because the T wave is very close to the QRS complex in rodents, the end of the QRS complex of each signal was considered to be the point at which the T wave started. Changes in the ST-T segment were measured by manual verification. Therefore, ST height represented the distance (in mV) from the baseline to the line where the T wave started (4).

Data analysis and statistics

All statistical analyses were performed using StatView software (Abacus Concept, Berkeley, CA, USA). The percentage change in diameter was calculated from the diameter change induced by an intervention as a percentage of the total amount of active tone (maximal diameter - baseline diameter). A plus value indicates vasodilation, and a minus value indicates vasoconstriction. A two-way ANOVA for repeated measures, followed by Tukey's post hoc test, was used to determine differences in vasodilation resulting from the various interventions. A one-way ANOVA was used to determine changes in biochemical data and fluorescence intensities,

followed by Tukey's test for multiple comparisons. A probability value of <0.05 was used to determine statistical significance.

Results

NO concentration induced by ACh and vitamin C level

We hypothesized that SMP30 deficiency decreases NO biosynthesis activity in the artery, because endothelium-dependent dilation, namely derived from NO, is an important mechanism of coronary flow regulation. Therefore we assessed the NO generation induced by acetylcholine (ACh, 1 μM) in the aorta of SMP30 KO and wild-type (WT) mice. The NO levels in the aortas of the SMP30 KO mice were lower than those of the WT mice (2.6±4.5 nM vs. 82.8±9.6 nM, n=10 each, P<0. 01) (Fig. 1). On the other hand, vitamin C levels in the aortas did not change between the SMP30 KO and WT mice (0.86±0.12 μmol/g tissue vs. 0.98±0.16 μmol/g tissue; n=10 each). These results suggest that SMP30 deficiency impairs NO biosynthesis from eNOS in the coronary artery, which is not dependent of the radical scavenging effect of vitamin C.

Concentration-dependent vasomotion of coronary arteries by ACh

We next assessed the coronary vascular response to ACh ($1x10^{-10\sim-5}$ M), which has endothelium-dependent vasodilative and vascular smooth muscle-dependent vasoconstrictive properties, in isolated pressurized coronary arteries of mice. In the SMP30 KO mice, ACh constricted the coronary arteries dose dependently (n=10, Fig. 2A). ACh-induced

vasoconstriction did not change with N^{ω}-nitro-L-arginine-methyl ester (L-NAME, 0.3 mM, *n*=10), a NOS inhibitor (Fig. 2A) or tetrahydrobiopterin (BH_4, 1 μM, *n*=10, Fig. 2B). With pretreatment of dithiothreitol (DTT, 0.1 μM), a thiol-reducing agent, the ACh response to coronary arteries changed from vasoconstriction to vasodilation in the SMP30 KO mice (*n*=10, *P*<0.01) (Fig. 2C). In the WT mice, ACh dilated coronary arteries dose dependently and ACh-induced vasodilation was blunted by L-NAME (*n*=10, each, Fig. 2A). ACh-induced vasodilation in the coronary arteries of WT mice decreased with pretreatment of 1, 3-bis (2-chloroethyl)-1-nitrosourea (BCNU, 80 μM), inhibitor of glutathione reductase (*n*=10, *P*<0.01), which was restored by DTT (*n*=10, Fig. 2D). Vasodilation of sodium nitroprusside (SNP, $1x10^{-10\sim-5}$ M), an endothelium independent vasodilator, was comparable between SMP30 KO and WT mice (*n*=10, each, Fig. 3). These results indicated that NOS activity was deteriorated in the coronary arteries with SMP30 deficiency. Redox signaling is a candidate for regulation of coronary vascular tone accompanied with thiol residue oxidation induced by ACh.

Generation of hydrogen peroxide (H_2O_2)

We assessed the H_2O_2 generation in the aorta of SMP30 KO and WT mice. SMP30 KO mice had a more than threefold increase in H_2O_2 levels of that measured in WT mice (18.1±1.8 vs. 4.6±0.7 pmol/mg protein/min

for SMP30 KO mice vs. WT mice, n=10 each, P<0.01, Fig. 4).

Concentration of asymmetric dimethylarginine (ADMA)

ADMA, an endogenous inhibitor of nitric oxide synthase, plays a pivotal role in endothelial dysfunction (23). Plasma and aorta ADMA levels were higher in SMP30 KO mice than WT mice (Plasma ADMA 1.3±0.1 vs. 0.7±0.1 nmol/mL, Fig. 5A; aorta ADMA 6.2±0.8 vs. 2.6±0.3 nmol/mL, n=10 each, P<0.01, respectively, Fig. 5B). These results suggest the possibility that SMP30 deficiency may impact L-arginine metabolism of eNOS and ADMA may contribute to the increase in superoxide generation.

Total thiol and glutathione levels in aorta

To determine how SMP30 deficiency affects thiols, total thiols and reduced (GSH) and oxidized glutathione (GSSG) levels were measured in aortic tissue of SMP30 KO and WT mice. In the aortic tissue of SMP30 KO mice, decreases of total thiols, GSH level, and GSH/GSSG with increase of GSSG level appeared compared to those in WT mice (total thiols 6.3±1.6 vs. 33.1±4.8 nmol/mg protein, Fig. 6A; GSH 5.1±0.8 vs. 18.6±2.1 nmol/mg protein, Fig. 6B; GSSG 1.9±0.3 vs. 1.1±0.2 nmol/mg protein, Fig. 6C; GSH/GSSG 2.8±0.5 vs. 14.8±1.8 in SMP30 KO mice vs. WT mice, n=10 each, P<0.01 respectively, Fig. 6D). From these results,

depletion of SMP30 may affect the total thiol level in the aortic tissue.

Generation of $O_2^{\cdot -}$ in coronary artery

As for the isolated coronary arteries, the production of superoxide anion radical ($O2^{\cdot -}$) was measured by staining with dihydroethidium (DHE 10 μM). We then examined reactive oxygen species (ROS) generation in the coronary arteries of the SMP30 KO mice with the hypothesis that SMP30 deficiency exacerbates ROS generation. The signal of DHE staining was enhanced in the coronary arteries with SMP30 deficiency [54±6.2 fluorescence intensity/100 μm^2 (Arbitrary Units), n=10] compared to that of WT mice (P<0.01). Apocynin (0.3 mM, n=10), an NADPH oxidase inhibitor, decreased this signal in the coronary arteries of the SMP30 KO mice (DHE 9.2±1.1 fluorescence intensitiy/100 μm^2, n=10 P<0.01 vs. without agent) (Fig. 7). This result suggests that superoxide generation in SMP30 deficiency depends on NADPH oxidase in the coronary arteries.

Oxidation of thiols in coronary arteries

To assess thiol oxidation in the coronary arteries, the location of thiols was determined by administration of fluorochrome monochlorobimane (MCB, 20 μM) or monobromotrimethylammoniobimane (MBB, 20 μM). Although these compounds covalently react with thiols, if the thiols are

oxidized, the compounds do not bind. Because MCB is permeable to the cell membrane and MBB is not, the total thiols and extracellular thiols can be respectively labeled. Thus, a reduction in fluorescence intensity means that thiols were oxidized, and that there was less binding of either fluorochrome (33). We investigated the modification of thiol oxidation by ACh (1 μM) and DTT (0.1 μM). ACh treatment decreased fluorescence levels due to MCB in the coronary arteries of the WT mice (MCB: 2.4±1.2 fluorescence intensity/100 μm^2, $P<0.01$ vs. without treatment, $n=10$, each). Fluorescence levels due to MCB or MBB in the coronary arteries decreased in the SMP30 KO mice (MCB 4.2±1.2, MBB 24±4.4 fluorescence intensity/100 μm^2, $n=10$ each, $P<0.01$, 0.05 vs. WT mice, respectively), and the level was restored with DTT treatment to a level comparable to that of the WT mice (SMP30 KO mice with DTT vs. WT mice: MCB 69±7.8 vs. 75±8.6, MBB 52±7.5 vs. 48±5.6, fluorescence intensity/100 μm^2, $n=10$, each). The degree of fluorescence intensity reduction with ACh in the coronary arteries was potent in MCB staining compared to that of MBB staining. These results suggest that total thiols were oxidized in the SMP30 KO mice. Elevation of fluorescence of MCB or MBB by DTT indicates reduction of oxidized thiols. Acetylcholine oxidized intracellular thiol with NO generation in WT mice coronary artery. Deficiency of SMP30 extinguishes additional thiol oxidation with ACh (Fig. 8A and B). Under high levels of total thiols and GSH as seen in WT mice artery, ACh can

release bioactive NO. However, deficiency of SMP30 shifts total thiols including glutathione reduced to oxidized, so ACh cannot release bioactive NO probably due to s-glutathionylation by oxidant stress in eNOS. From these results, we speculate that total thiol oxidation makes generation of bioactive NO in eNOS difficult.

ST-T segment change in electrocardiogram

Finally, we examined whether intra-aortic sinus administration of ACh induces coronary artery spasm in SMP30 KO mice. We determined that administration of 2 μg ACh is a suitable dose for examination of coronary artery response in the *in vivo* condition. The duration and magnitude of the ST-T segment change by administration of 0.2 μg ACh were too small. Also, the administration of 20 μg ACh decreased the blood pressure to 72±8% as well as bradycardia. We thus administered 2 μg ACh to determine the effect of ACh on the ST-T segment change in electrocardiogram. In the SMP30 KO mice, ischemic ST-T segment elevation appeared from 30 sec to 1 min after ACh administration [0.35±0.06 mV (0.2-0.5 mV)] with reciprocal ST-T segment depression, and spontaneously returned to the baseline after around 2 min. In the WT mice, the ST-T segment did not change with ACh administration (Fig. 9A and B). These results implied that SMP30 KO mouse is a suitable model for the investigation of coronary artery spasm.

Discussion

To our knowledge, this is the first study indicating that thiol oxidation inhibits nitric oxide production and causes coronary artery spasm under SMP 30 deficiency. The new findings bear on the understanding of the mechanisms by which thiol-oxidation modifies coronary artery tone, and reveal how age-associated oxidant stress is a major risk factor of coronary vasospasm. First of all, coronary artery vasoconstriction or vasodilation is redox sensitive. A large fluorescent signal from either MCB or MBB in coronary arteries and high levels of total thiol and GSH in aorta appeared in WT mice. On the other hand, the signal for MCB was reduced in the coronary arteries of SMP30 KO mice (nearly eliminated), even more than for MBB with decreases of GSH and total thiols in the aorta. This suggests that the largest component of thiols oxidized (and thus less binding) is intracellular. The principal decrease of fluorescence was prevented or attenuated by DTT. Moreover, vasoconstriction in SMP30 KO mice coronary arteries induced by ACh, that is widely used to investigate the bioavailability of nitric oxide and coronary artery spasm in clinical setting (2), was inhibited by DTT. BCNU, an inhibitor of glutathione reductase, attenuated vasodilation induced by ACh in WT mice coronary arteries, which was reversed by DTT.

These results suggest that the redox condition of intracellular thiols

mediates coronary vasospasm. Second, SMP30 has a protective action against oxidant damage that does not influence antioxidant enzyme status (36). Increased levels of reactive oxygen species, emphasized NADPH oxidase, and myeloperoxidase activities appeared in SMP30 KO mice (37). Therefore, SMP30 KO mice are suitable chronic oxidant stress models. Deficiency of SMP30 has a deletion of vitamin C biosynthesis (37). In this study, we fed vitamin C including chow, and the level of vitamin C was not different among SMP30 KO and WT mice. Thus, the ACh-induced vascular response is unaffected by the level of vitamin C. However, the long-term effect of vitamin C treatment remains unknown because of previous data suggesting that there was improvement of NOS activity with an overdose chronic administration of vitamin C (8). Thus, further study is needed to clarify the effect of vitamin C on thiol oxidation.

Taken together, our results support the conclusion that redox-dependent vasoconstriction has an important role in the pathogenesis of coronary artery spasm that comes with aging. The present data are supported by a number of previous observations. NO synthesized in the presence of L-arginine and BH_4 in eNOS has a critical role in the regulation of vascular function (31, 40). In the absence of BH_4, NO synthesis is abrogated and superoxide is generated instead. While NO dysfunction occurs increasingly with redox stresses like aging, BH_4 repletion only partly restores NOS activity and NOS-dependent vasodilation (9). It appeared in this study that

pretreatment of BH_4 did not attenuate ACh-induced vasoconstriction *in vitro*. Accordingly, coronary vasospasm in SMP30 KO mice induced by ACh is not due to the deletion of BH_4. Protein thiol can undergo thiol oxidation, a reversible protein modification involved in cellular signaling and adaptation (12). Under oxidant stress, thiol oxidation like s-glutathionylation in cysteine residues, which are critical for maintenance of eNOS function, occurs through a thiol-disulfide exchange with GSSG, which can only occur when the cellular GSH/GSSG ratio is low as shown in SMP30 KO mice (3, 11, 41), or a reaction of oxidant-induced protein thiyl radicals with reduced glutathione (45).

Recently, it has been reported that s-glutathionylation of eNOS reversibly decreases NOS activity with an increase in superoxide generation primarily from reductase. In this state, two highly conserved cysteine residues are identified as sites of s-glutathionylation, and found to be critical for redox-regulation of eNOS function (6). It has been reported that GSH synthase inhibition without oxidation by buthionine-(*S, R*)-sulfoximine had no effect on NO bioactivity (16). However, thiol depletion *in vivo* greatly reduces NO generation from eNOS (7, 14, 15). Decrease of NO bioactivity with GSH depletion under oxidant stress has been reported (44), and thiol oxidizing agent like diamide decreased both GSH level and NO bioactivity (16). Therefore, we speculate that decreases of GSH and total thiols including cysteine residues in eNOS domain by oxidative stress may

contribute to impairment of NO generation in SMP30 KO mice. However, the possibility that ADMA, which increased in plasma and aortic tissue of SMP30 KO mice, has a role in the deterioration of endothelium dependent vasodilation under SMP30 deficiency cannot be ruled out.

Although the main source of superoxide production in SMP30 KO mice coronary arteries is undefined, we speculate that it is an NAD(P)H oxidase-dependent $O_2^{\cdot -}$ production. There is increasing evidence that NAD(P)H oxidase is a major source of $O_2^{\cdot -}$ in the vasculature, and that $O_2^{\cdot -}$ from this enzyme serves as an important physiological redox signaling molecule, participating in the regulation of vascular function associated with a novel Ca^{2+} signaling pathway (13, 29, 47). In addition, deficiency of SMP30, also reported as a regucalcin, induces the lack of vitamin C biosynthesization, impairs the scavenging effect of reactive oxygen species, and increases the NADPH oxidase activity in vessels (22, 42). From this evidence, we propose that an augmentation of NADPH oxidase activity might trigger an increase in intracellular Ca^{2+} stress. This will lead to coronary vasospasm in SMP30 KO model, though further study is needed.

A limitation of our present study is that we did not observe coronary angiograms during vasospasm attacks, although ischemic ST-T elevation and reciprocal ST-T segment depression in electrocardiograms were transient and sodium nitroprusside was effective in releasing ST-T segment change. Moreover, similar transient ST-T segment change appeared with

intravenous administration of 5-hydroxytryptamine (data not shown). Thus, it is possible that the coronary artery spasm in this model is constant, not provocatively agent-dependent. Therefore, SMP30 KO mouse may be a useful model to investigate oxidant stress-mediated coronary artery spasm.

Calcium antagonists are generally first choice for patients with coronary artery spasm in the clinical setting. However, the effect is partial, especially in elderly patients. Recently, oxidant stress is considered to play an important role in the occurrence of coronary artery spasm. Considering the results of our study, thiol oxidation with chronic oxidant stress may play a key role in age-related coronary artery spasm (Fig. 10). Thus, further improvement of antioxidant therapy will lead to effective therapy of coronary artery spasm.

In conclusion, thiol oxidation is a pivotal switch for inducing endothelial dysfunction and coronary artery spasm, providing a redox modification of the coronary vascular tone in aging.

Acknowledgments

This study was supported in part by grants-in-aid for Scientific Research (Nos. 21590935 and 24591100) from the Japan Society for the Promotion of Science.

References

1. Baker MA, Cerniglia GJ, and Zaman A. Microtiter plate assay for the measurement of glutathione and glutathione disulfide in large numbers of biological samples. *Anal Biochem* 190: 360–365, 1990.
2. Beltrame JF, Sasayama S, and Maseri A. Racial heterogeneity in coronary artery vasomotor reactivity: Differences between Japanese and Caucasian patients. *J Am Coll Cardiol* 33: 1442-1452, 1999.
3. Biswas S, Chida AS, and Rahman I. Redox modifications of protein-thiols: emerging roles in cell signaling. *Biochem Pharmacol* 71: 551-564, 2006.
4. Bostick B, Yue Y, and Duan D. Phenotyping cardiac gene therapy in mice. *Methods Mol Biol* 709: 91–104, 2011.
5. Cai H, McNally JS, Weber M, and Harrison DG. Oscillatory shear stress upregulation of endothelial nitric oxide synthase requires intracellular hydrogen peroxide and CaMKII. *J Mol Cell Cardiol* 37: 121–125, 2004.
6. Chen CA, Wang TY, Varadharaj S, Reyes LA, Hemann C, Talukder MAH, Chen YR, Druhan LJ, and Zweier JL. S-glutathionylation uncouples eNOS and regulates its cellular and vascular function. *Nature* 468: 1115-1121, 2010.
7. Cuzzocrea S, Zingarelli B, O'Connor M, Salzman AL, and Szabó C. Effect of L-buthionine-(S,R)-sulphoximine, an inhibitor of gamma-glutamylcysteine synthetase on peroxynitrite- and endotoxic shock-induced vascular failure. *Br J Pharmacol* 123:525-537, 1998.
8. d'Uscio LV, Milstien S, Richardson D, Smith R, and Katusic Z. Long-term vitamin C treatment increases vascular tetrahydrobiopterin levels and nitric oxide synthase activity. *Circ Res* 92: 88-95, 2003.
9. Dumitrescu C, Biondi R, Xia Y, Cardounel AJ, Druhan LJ, Ambrosio G, and Zweier JL. Myocardial ischemia results in tetrahydrobiopterin (BH4) oxidation with impaired endothelial function ameliorated by BH4. *Pro Natl Aca Sci USA* 104: 15081-15086, 2007.
10. Finkel T and Holbrook NJ. Oxidants, oxidative stress and the biology of ageing. *Nature* 408: 239-47, 2000.

11. Gallogly MM and Mieyal JJ. Mechanisms of reversible protein glutathionylation in redox signaling and oxidative stress. *Curr Opin Pharmacol* 7: 381-391, 2007.
12. Glustarini D, Rossi R, milzani A, Colombo R, and Dalle-Donne I. S-glutathionylation: from redox regulation of protein functions to human disease. *J Cell Mol Med* 8: 201-212, 2004.
13. Griendling KK, Sorescu D, and Ushio-Fukai M. NAD(P)H oxidase: role in cardiovascular biology and disease. *Circ Res* 86: 494-501, 2000
14. Harbrecht BG, Di Silvio M, Chough V, Kim YM, Simmons RL, and Billiar TR. Glutathione regulates nitric oxide synthase in cultured hepatocytes. *Ann Surg* 225: 76-87, 1997.
15. Hothersall JS, Cunha FQ, Neild GH, and Norohna-Dutra AA. Induction of nitric oxide synthesis in J774 cells lowers intracellular glutathione: effect of modulated glutathione redox status on nitric oxide synthase induction. *Biochem J* 322: 477-481, 1997.
16. Huang A, Xiao H, Samii JM, and Vita JA. Contrasting effects of thiol-modulating agents on endothelial NO bioactivity. *Am J Physiol Cell Physiol* 281: C719-C725, 2001.
17. Ishigami A, Fujita T, Handa S, Shirasawa T, Koseki H, and Kitamura T. Senescence marker protein-30 knock-out mouse liver is highly susceptible to tumor necrosis factor-alpha and Fas-mediated apotosis. *Am J Pathol* 16: 1273-1281, 2002.
18. Iwama M, Shimokado K, Maruyama N, and Ishigami A. Time course of vitamin C distribution and absorption after oral administration in SMP30/GNL knockout mice. *Nutrition* 30: 40916, 2010.
19. Kashio Amano A, Kondo Y, Sakamoto T, Iwamura H, Suzuki M, Ishigami A, and Yamasoba T. Effect of vitamin C depletion on age-related hearing loss in SMP30/GNL knockout mice. *Biochem Biophys Res Commun* 390: 394-398, 2009.
20. Kondo Y, Sasaki T, Sato Y, Amano A, Aizawa S, Iwama M, Handa S, Shimada N, Fukuda M, Akita M, Lee J, Jeong KS, Maruyama N, and Ishigami A. Vitamin C depletion increases superoxide generation in brains of SMP30/GNL knockout mice. *Biochem Biophy Res Comm* 377: 291-296, 2008.
21. Kugiyama K, Ohsugi M, Motoyama T, Sugiyama S, Ogawa H, Yoshimura M, Inobe Y, Hirashima O, Kawano H, Soejima H, and Yasue H. Nitric oxide-mediated

flow-dependent dilation is impaired in coronary arteries in patients with coronary spastic angina. *J Am Coll Cardiol* 30: 920-926, 1997.

22. Lai P, Yip NC, and Michelangeli F. Regucalcin (RGN/SMP30) alters agonist– and thapsigagin–induced cytosolic [Ca2+] transients in cells by increasing SERCA Ca^{2+} ATPase levels. *FEBS Lett* 585: 142902, 2011.
23. Li Volti G, Salomone S, Sorrenti V, Mangiameli A, Urso V, Siarkos I, Galvano F, and Salamone F. Effect of silibinin on endothelial dysfunction and ADMA levels in obese diabetic mice. *Cardiovasc Diabetol* 10: 62, 2011.
24. Machii H, Saitoh S, Kaneshiro T, and Takeishi Y. Aging impairs myocardium-induced dilation in coronary arterioles: Role of hydrogen peroxide and angiotensin. *Mech Age Dev* 131: 710-717, 2010.
25. Maekawa K, Kawamoto K, Fuke S, Yoshioka R, Saito H, Saito T, and Hioka T. Images cardiovascular medicine. Severe endothelial dysfunction after sirolimus-eluting stent implantation. *Circulation* 113: e850-e851, 2006.
26. Mingone CJ, Gupte SA, Ali N, Oeckler RA, and Wollin MS. Thiol oxidation inhibits nitric oxide-mediated pulmonary artery relaxation and guanylate cyclase stimulation. *Am J Physiol Lung Cell Mol Physiol* 290: l549-1557, 2006.
27. Miwa K, Kishimoto C, Nakamura H, Makita T, Ishii K, Okuda N, Taniguchi A, Shioji K, Yodoi J, and Sasayama S. Increased oxidative stress with elevated serum thioredoxin level in patients with coronary spastic angina. *Clin Cardiol* 26: 177-181, 2003.
28. Miyata K, Shimokawa H, Yamawaki T, Kunihiro I, Zhou X, Higo T, Tanaka E, Katsumata N, Egashira K, and Takeshita A. Endothelial vasodilator function is preserved at the spastic/inflammatory coronary lesions in pigs. *Circulation* 100: 1432-1437, 1999.
29. Mohazzab KM and Wolin MS. Sites of superoxide anion production detected by lucigenin in calf pulmonary artery smooth muscle. *Am J Physiol Lung Cell Mol Physiol* 267: L815-L8222, 1994.
30. Moukarbel GV and Dakik HA. Diffuse coronary artery spasm induced by guidewire insertion. *J Invasive Cardiol* 15: 353-354, 2003.
31. Palmer RM, Ashton DS, and Moncada S. Vascular endothelial cells synthesize nitric oxide from L-arginine. *Nature* 333: 664-666, 1988.

32. Picchi A, Gao X, Belmadani S, Potter BJ, Focardi M, Chilian WM, and Zhang C. Tumor necrosis factor-α induces endothelial dysfunction in the prediabetic metabolic syndrome. *Circ Res* 99: 69-77, 2006.
33. Saitoh S, Kiyooka T, Rocic P, Rogers PA, Zhang C, Swafford A, Dick GM, Viswanathan C, Park Y, and Chilian WM. Redox-dependent coronary metabolic dilation. *Am J Physiol Heart Circ Physiol* 293: H3720-H3725, 2007.
34. Saitoh S, Zhang C, Tune JD, Potter B, Kiyooka T, Rogers PA, Knudson JD, Dick GM, Swafford A, and Chilian WM. Hydrogen peroxide: A feed-forward dilator that couples myocardial metablism to coronary flow. *Arterioscler Thromb Vasc Biol* 26: 2614-2621, 2006.
35. Shimokawa H. Cellular and molecular mechanisms of coronary artery spasm. *Jpn Circ J* 64: 1-12, 2000.
36. Son TG, Kim SJ, Kim K, Kim MS, Chung HY, and Lee J. Cytoprotective roles of senescence marker protein 30 against intracellular calcium elevation and oxidative stress. *Arch Pharm Res* 31: 872-877, 2008.
37. Son TG, Zou Y, Jung KJ, Yu BP, Ishigami A, Maruyama N, and Lee J. SMP30 deficiency causes increased oxidant stress in brain. *Mech Age Dev* 127: 451-457, 2006.
38. Teragawa H, Kato M, Kurosawa J, Yamagata T, Matsuura H, and Chayama K. Endothelial dysfunction is an independent factor responsible for vasospastic angina. *Clin Sci (Lond)* 101: 707-713, 2001.
39. Weiss N, Heydrick S, Zhang YY, Bierl C, Cap A, and Loscalzo J. Cellular redox state and endothelial dysfunction in mildly hyperhomocysteinemic cystathionine β -synthase –deficient mice. *Arterioscler Thromb Vasc Biol* 22: 34-41, 2002.
40. Werner ER, Gorren AC, Heller R, Werner-Felmayer G, and Mayer B. Tetrahydrobiopterin and nitric oxide: mechanistic and pharmacological aspects. *Exp Biol Med* 228: 1291-1300, 2003.
41. Winterbourn CC and Hampton MB. Thiol chemistry and specificity in redox signaling. *Free Radic Biol Med* 45:549-561, 2008.
42. Wison JX and Wu F. Vitamin C in sepsis. *Subcell Biochem* 56: 67-83, 2012.
43. Yamaguchi O, Kaneshiro T, Saitoh S, ishibashi T, Maruyama Y, and Takeishi Y. regulation of coronary vascular tone via redox modulation in the

α1-adrenergic-angiotensin-endothelin-axis of the myocardium. *Am J Physiol Heart Circ Physiol* 296: H226-H232, 2009.

44. Yan J, Tie G, and Messina LM. Tetrahydrobiopterin, L-arginine and vitamin C act synergistically to decrease oxidative stress, increase nitricoxide and improve blood flow after induction of hindlimb ischemia in the rat. *Mol Med* 18: 676-684, 2012.
45. Ying J, Clavreul N, Sethuraman M, Adachi T, and Cohen RA. Thiol oxidation in signaling and response to stress detection and quantification of physiological and pathophysiological thiol modifications. *Free Radic Biol Med* 43: 1099-1108, 2006.
46. Zima AV and Blatter LA. Redox regulation of cardiac calcium channels and transporters. *Cardiovasc Res* 71: 310-321, 2006.
47. Zulueta JJ, Yu FS, Hertig IA, Thannickal VJ, and Hassoun PM. Release of hydrogen peroxide in response to hypoxia-reoxygenation: role of an NAD(P)H oxidase-like enzyme in endothelial cell plasma membrane. *Am J Respir Cell Mol Biol* 12: 41-49, 1995.
48. Fujita T, Uchida k, Maruyama N. Purification of senescence marker protein-30 (SMP30) and its independent decreases with age in the rat liver. *Biochem Biophys Acta* 1992; 1116: 122-128.

Figure Legends

FIG. 1. **Nitric oxide (NO) generation in aorta.** Representative electrochemical detection tracing of NO concentration in isolated aortas from the SMP30 KO and WT mice in an organ chamber. NO concentration is directly proportional to the current (pA) by free radical analyzer (Apollo 4000). ACh (1 μM)-stimulated NO release was attenuated in SMP30 KO mice vs. WT mice ($p<0.01$). ACh indicates acetylcholine administration.

FIG. 2. Isolated coronary artery responses to ACh ($1x10^{-10\sim5}$ M) in SMP30 KO and WT mice in organ chamber. ACh-induced vasoconstriction appeared in the SMP30 KO mice. The NOS inhibitor, L-NAME (0.3 mM), did not further enhance this response. In the WT mice, ACh-induced vasodilation appeared, blunted with L-NAME **(A)**. BH_4 (1 μM) did not change ACh-induced vasoconstriction in the SMP30 KO mice **(B)**. ACh-induced vasoconstriction in the SMP30 KO mice changed to vasodilation with the thiol-reducing agent, DTT (0.1 μM) **(C)**. Inhibition of glutathione reductase with BCNU (80 μM) decreased ACh-induced vasodilation, which was restored by DTT in the WT mice **(D)**. Values were expressed as means ± S.E.M. $n=10$, each, * $p<0.01$.

FIG. 3. Sodium nitroprusside (SNP) response in isolated coronary

arteries from SMP30 KO and WT mice in organ chamber. SNP ($1x10^{-10\sim-5}$ M) induced vasodilation dose-dependently, which was comparable between the SMP30 and WT mice. Values were expressed as means ± S.E.M. *n*=10, each.

FIG. 4. Hydrogen peroxide (H_2O_2) generation in the aorta. H_2O_2 production determined by Amplex-Red assay in the aortic tissue of WT and SMP30 KO mice. SMP30 KO mice had a more than threefold increase in H_2O_2 levels. Values were expressed as means ± S.E.M. *n*=10, each, * $p<0.01$.

FIG. 5. Plasma and aorta asymmetric dimethylarginine (ADMA) levels. Plasma ADMA was higher in SMP30 KO mice than WT mice **(A)**. Aorta ADMA was similarly higher in SMP30 KO mice **(B)**. Values were expressed as means ± S.E.M. *n*=10, each, * $p<0.01$.

FIG. 6. Aortic tissue total thiols and glutathione levels In aortic tissue, the levels of total thiols (A) and of reduced glutathione (GSH) (B) decreased in SMP30 KO mice compared to those in WT mice. In contrast, the level of oxidized glutathione (GSSG) increased in SMP30 KO mice (C). Deficiency of SMP30 led to a decrease in the ratio of reduced to oxidized glutathione (GSH/GSSG) (D). Values were expressed as means ± S.E.M.

n=10, each, * p<0.01.

FIG. 7. DHE staining in coronary arteries. Production of superoxide anion radical was measured by staining with 10 μM DHE in the isolated coronary arteries. **Upper panel** shows representative DHE and the **lower panel** shows summary data of DHE fluorescent intensity (in arbitrary units) in the coronary arteries. The signal of DHE was potent with SMP30 deficiency, which was attenuated with apocynin (0.3 mM). Values were expressed as means±S.E.M. * p<0.01 vs. without any treatment in WT mice, $^{\#}$ p<0.01 vs. without treatment in SMP30 KO mice. n=10, each.

FIG. 8. Oxidation of thiols in coronary arteries. We investigated the modification of thiol oxidation with ACh (1 μM) or DTT (0.1 μM) in isolated the coronary arteries. Total or extracellular thiols were labeled with either MCB (20 μM, **A)** or MBB **(**20 μM**, B)**, respectively. **Upper panels** show fluorescent images of total reduced or extracellular reduced free thiol groups and the **lower panels** show summary data of fluorescent intensity (in arbitrary units) in isolated coronary arteries. A decrease in fluorescence indicates thiol oxidation with less binding of either fluorochrome. Fluorescence from MCB or MBB was decreased (increased thiol oxidation) in SMP30 KO mice compared to those of the WT mice. Acetylcholine decreased MCB signal in the coronary arteries of the WT mice.

Fluorescence to either indicator increased after administration of DTT (0.1 μM). Decrease of fluorescent intensity was greater in MCB than in MBB of the SMP30 KO mice, indicating the effect on intracellular thiol oxidation. Values were expressed as means ± S.E.M. n=10, each. * p<0.01, **p<0.05 vs. without any treatment of WT mice. $^{\#}p$<0.01, $^{\#\#}p$<0.05 vs. without any treatment of SMP30 KO mice.

FIG. 9. Acetylcholine-induced coronary artery spasm. Intra-aortic sinus administration of ACh (2 μg) to the SMP30 KO mice induced transient ST-T segment elevation and reciprocal ST-T segment depression in electrocardiogram **(A)**. In the WT mice, ACh-induced ST-T segment change did not appear (**B**). Before, after 1, 2, and 5 min; before, after 1, 2, and 5 min intra-aortic sinus administration of ACh, respectively.

FIG. 10. Thiol oxidation in the coronary arteries. Increase in reactive oxygen species, through NADPH oxidase activation with the senescence marker protein-30 deficiency, induces thiol oxidation in endothelial nitric oxide synthase, and finally attenuates bioactive nitric oxide generation in endothelial cells. ACh: acetylcholine, SMP30: senescence marker protein-30, ROS: reactive oxygen species, eNOS: endothelial nitric oxide synthase, L-Arg: L arginine, NO: nitric oxide, ADMA: asymmetric dimethylarginine

FIG. 1.

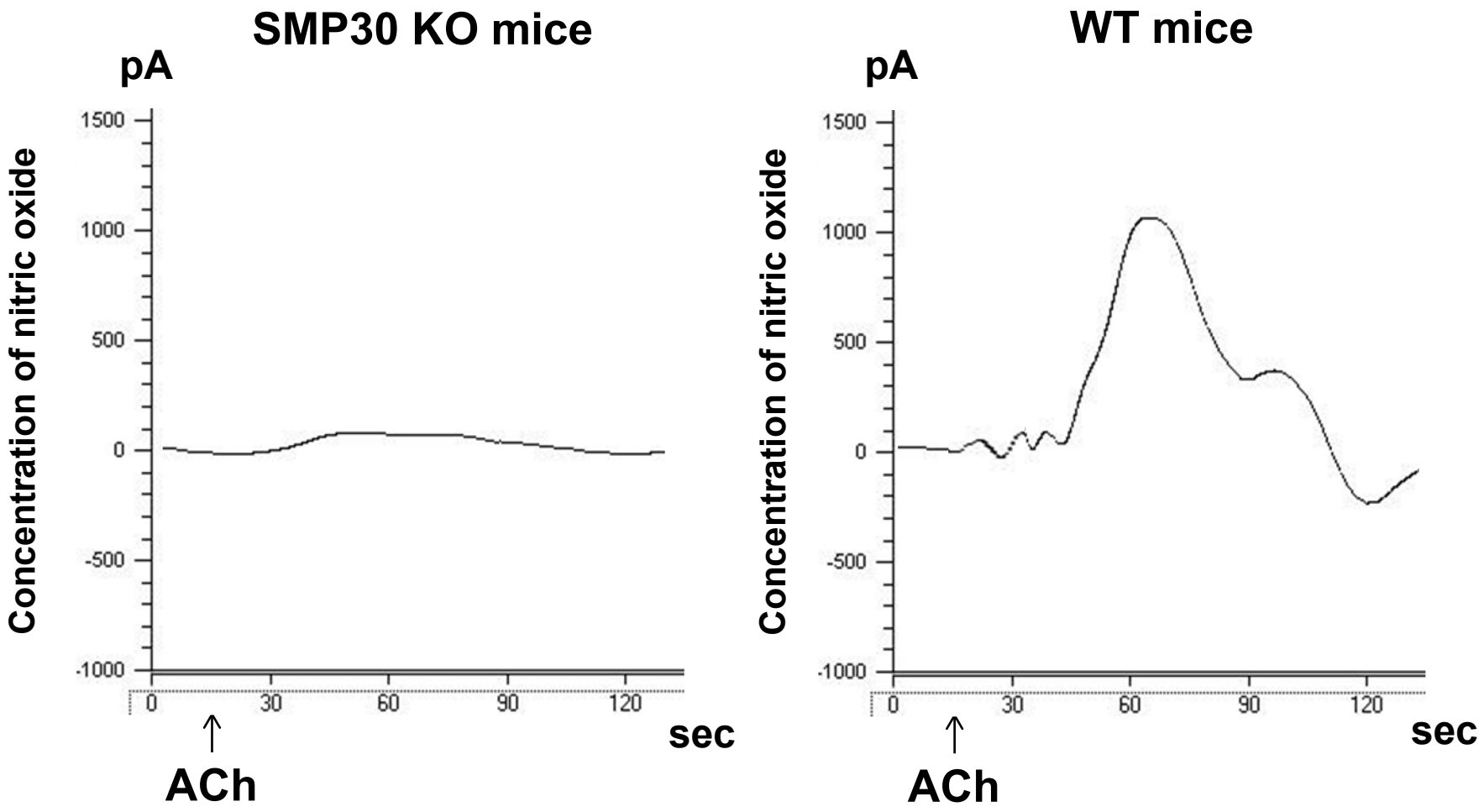
SMP30 KO mice
pA
Concentration of nitric oxide
1500
1000
500
0
-500
-1000
0
30
60
90
120
sec
ACh
WT mice
pA
Concentration of nitric oxide
1500
1000
500
0
-500
-1000
0
30
60
90
120
sec
ACh

FIG. 2.

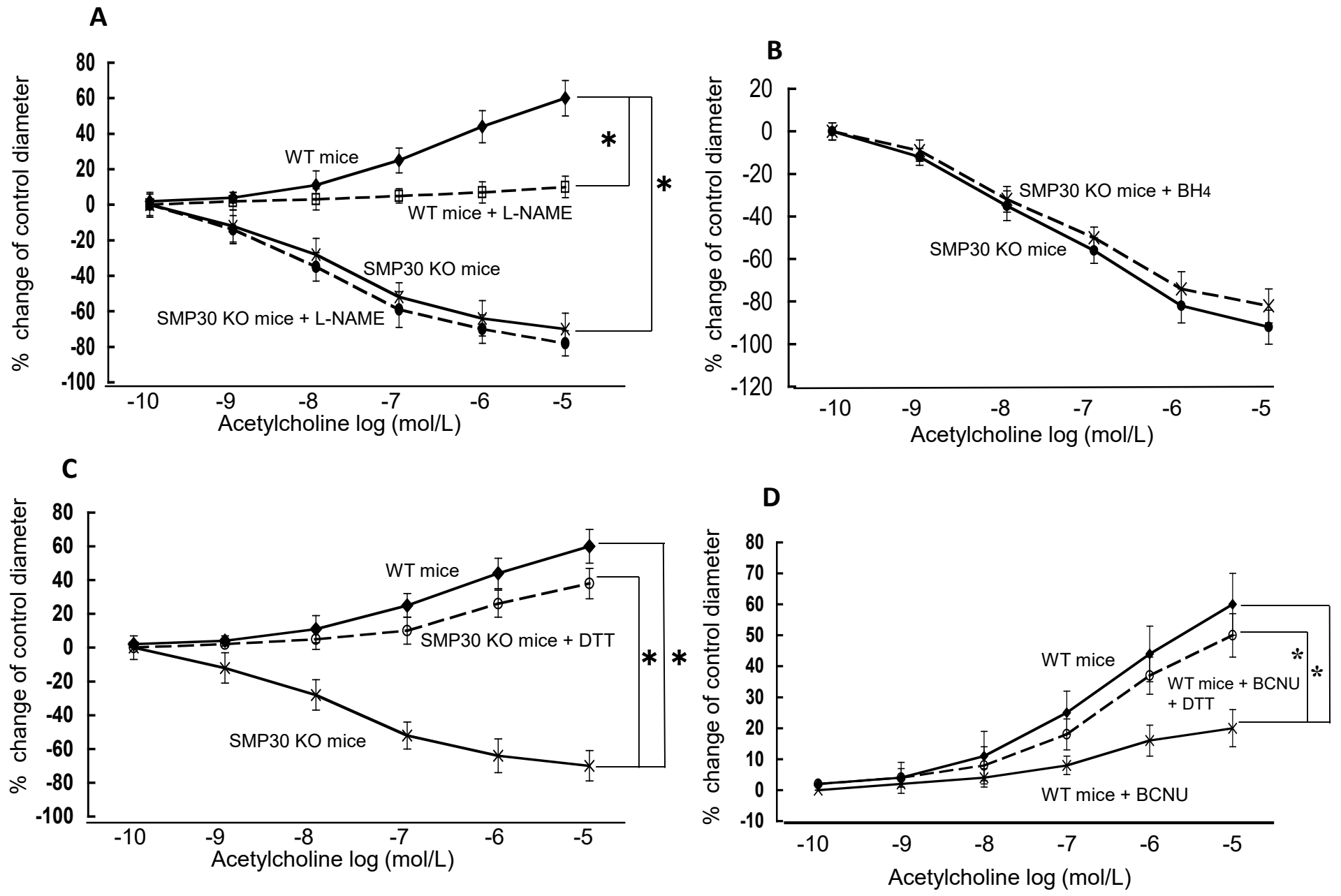
A
% change of control diameter
80
60
40
20
0
-20
-40
-60
-80
-100
WT mice
WT mice + L-NAME
SMP30 KO mice
SMP30 KO mice + L-NAME
*
*
-10
-9
-8
-7
-6
-5
Acetylcholine log (mol/L)
B
% change of control diameter
20
0
-20
-40
-60
-80
-100
-120
SMP30 KO mice + BH4
SMP30 KO mice
-10
-9
-8
-7
-6
-5
Acetylcholine log (mol/L)
C
% change of control diameter
80
60
40
20
0
-20
-40
-60
-80
-100
WT mice
SMP30 KO mice + DTT
SMP30 KO mice
*
*
-10
-9
-8
-7
-6
-5
Acetylcholine log (mol/L)
D
% change of control diameter
80
70
60
50
40
30
20
10
0
-10
WT mice
WT mice + BCNU + DTT
WT mice + BCNU
*
*
-10
-9
-8
-7
-6
-5
Acetylcholine log (mol/L)

FIG. 3.

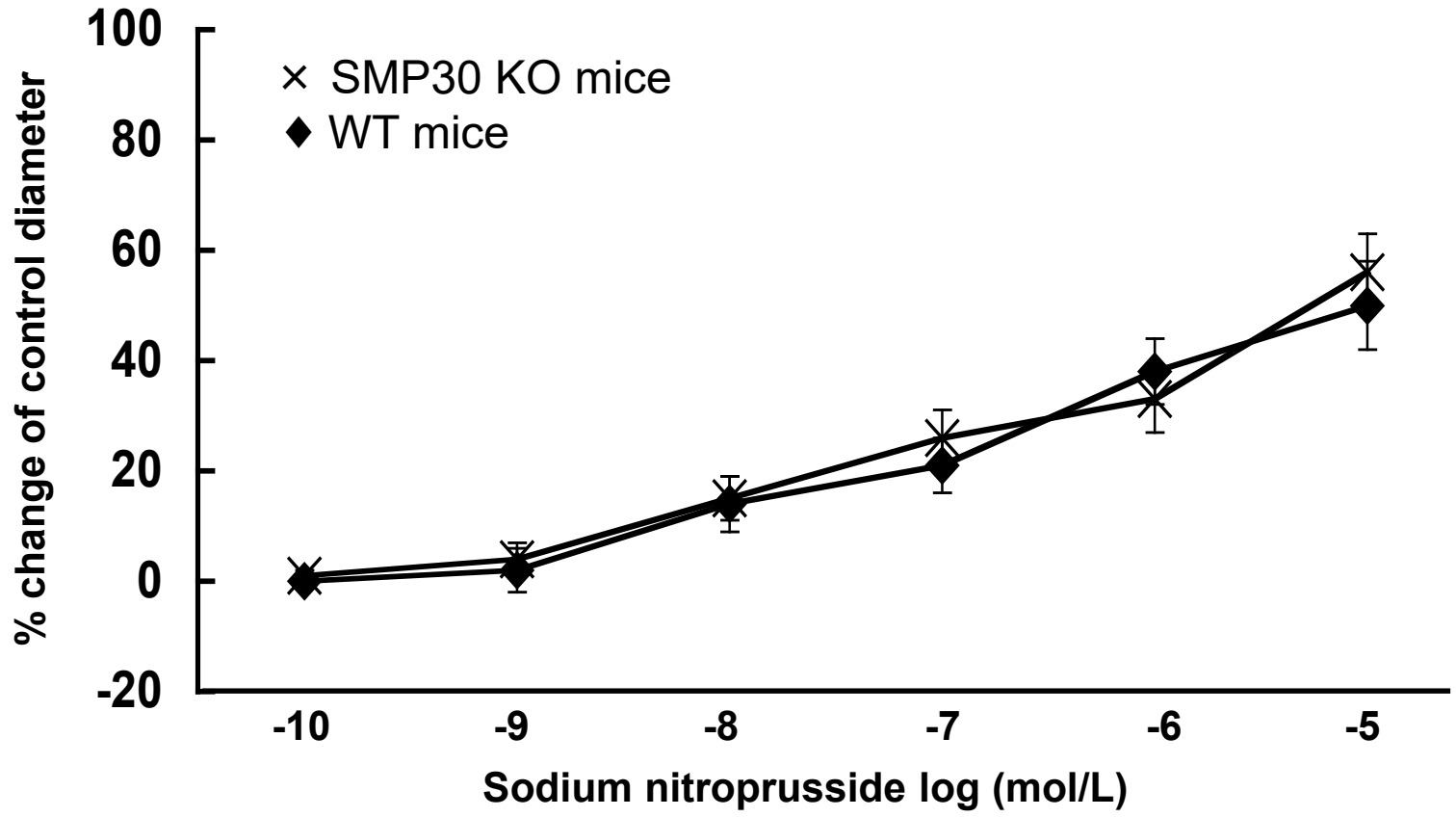
100
80
60
40
20
0
-20
% change of control diameter
× SMP30 KO mice
◆ WT mice
-10
-9
-8
-7
-6
-5
Sodium nitroprusside log (mol/L)

FIG. 4.

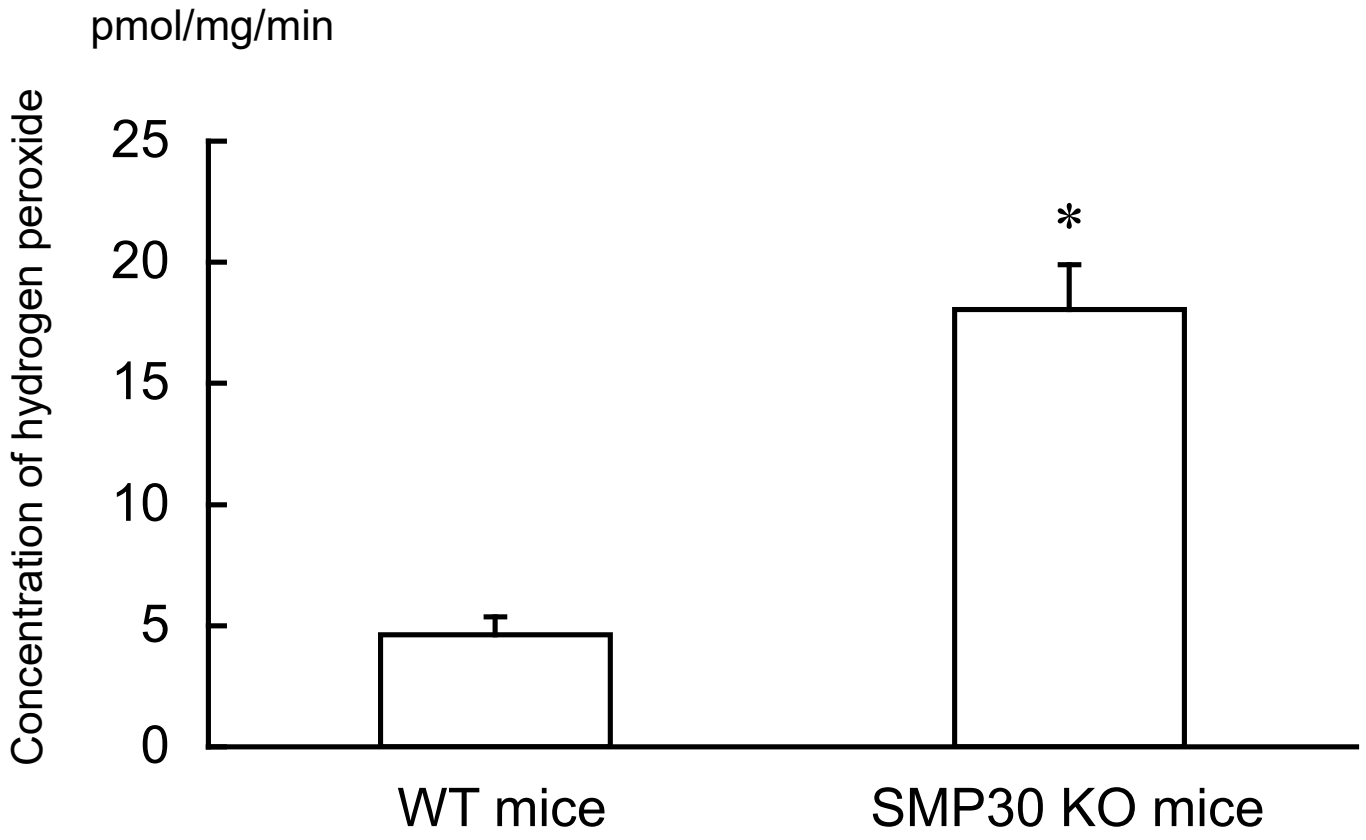
pmol/mg/min
Concentration of hydrogen peroxide
25
20
15
10
5
0
*
WT mice
SMP30 KO mice

FIG. 5.

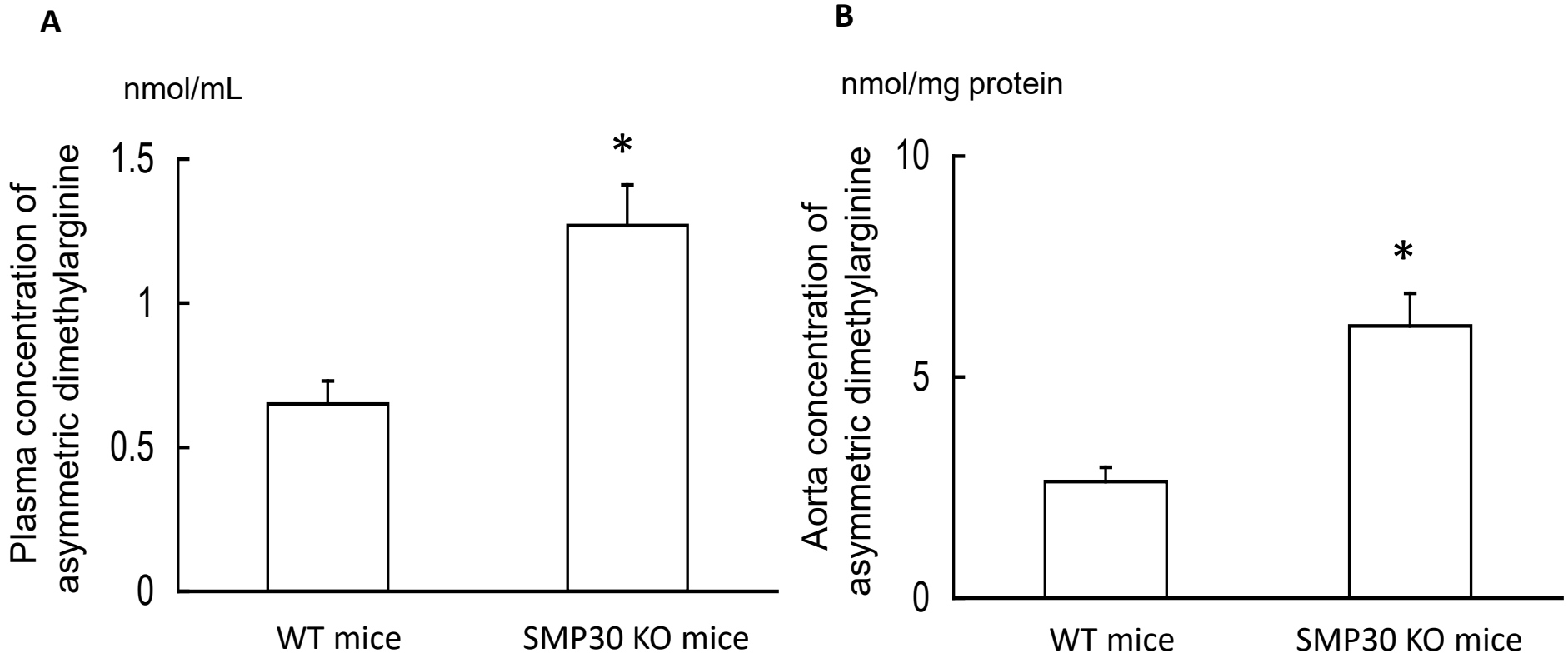
A
nmol/mL
Plasma concentration of asymmetric dimethylarginine
1.5
1
0.5
0
*
WT mice
SMP30 KO mice
B
nmol/mg protein
Aorta concentration of asymmetric dimethylarginine
10
5
0
*
WT mice
SMP30 KO mice

FIG. 6.

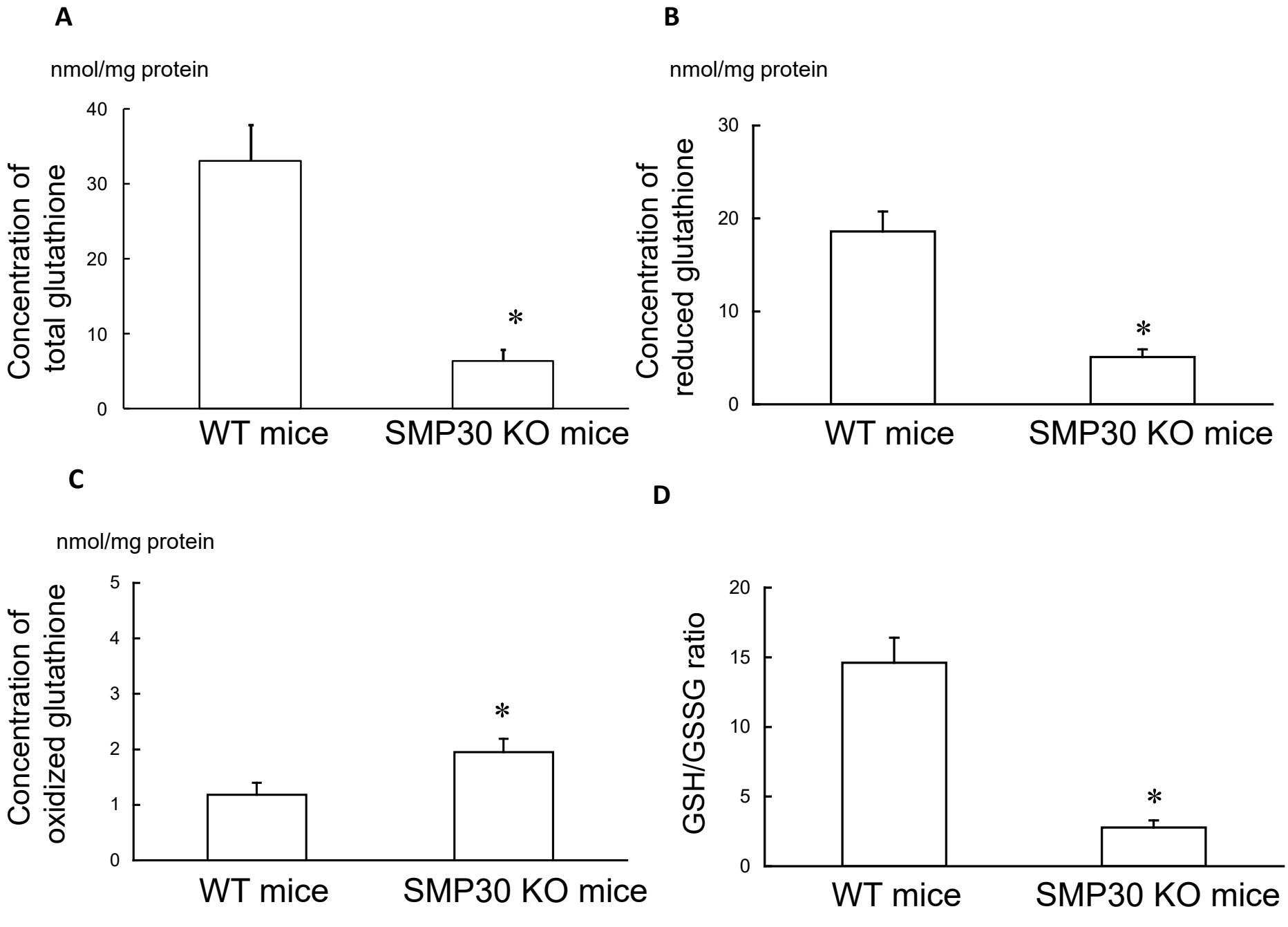
A
nmol/mg protein
Concentration of total glutathione
40
30
20
10
0
*
WT mice
SMP30 KO mice
B
nmol/mg protein
Concentration of reduced glutathione
30
20
10
0
*
WT mice
SMP30 KO mice
C
nmol/mg protein
Concentration of oxidized glutathione
5
4
3
2
1
0
*
WT mice
SMP30 KO mice
D
GSH/GSSG ratio
20
15
10
5
0
*
WT mice
SMP30 KO mice

FIG. 7.

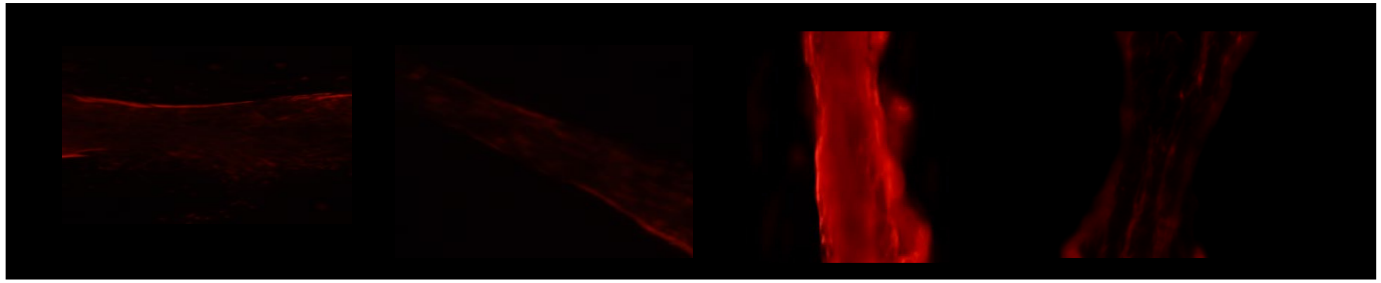

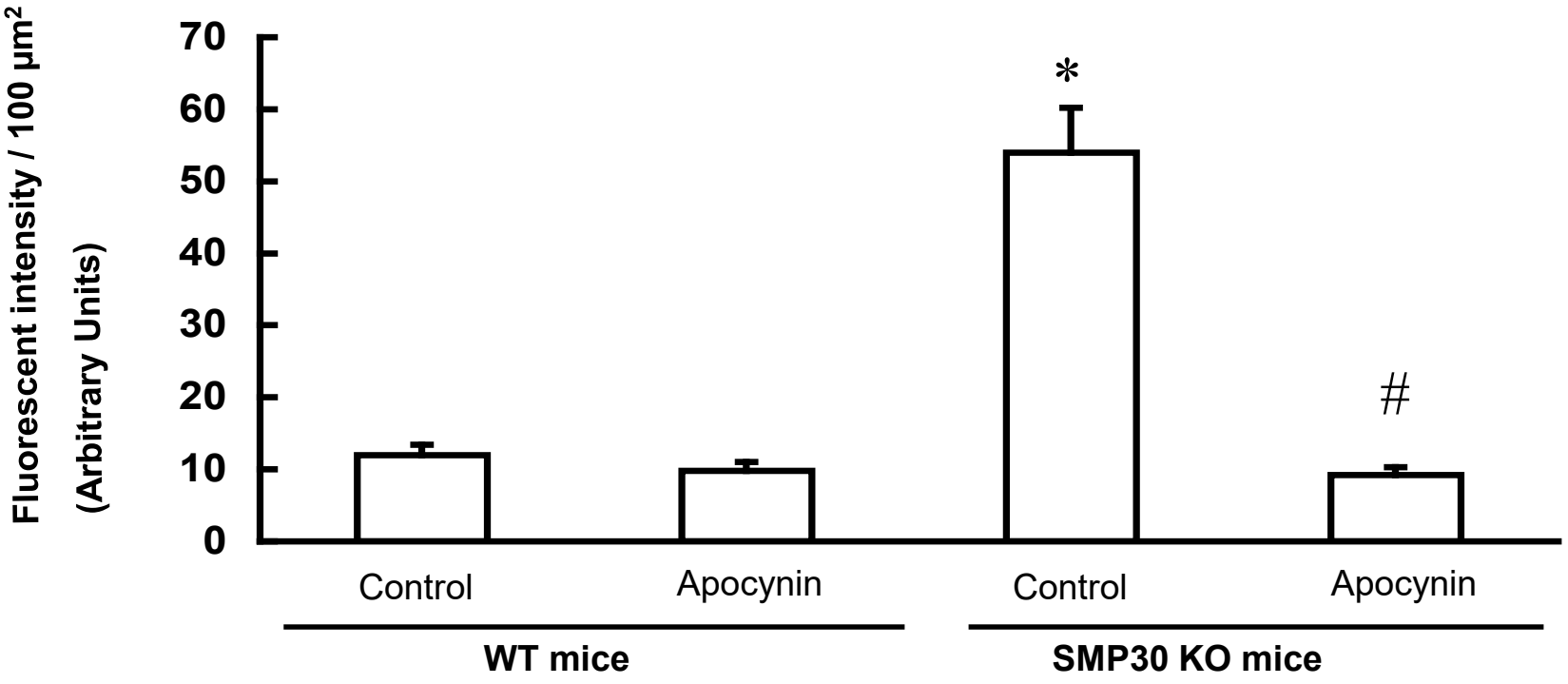
Fluorescent intensity / 100 μm²
(Arbitrary Units)
70
60
50
40
30
20
10
0
*
#
Control
Apocynin
Control
Apocynin
WT mice
SMP30 KO mice

FIG. 8.

A

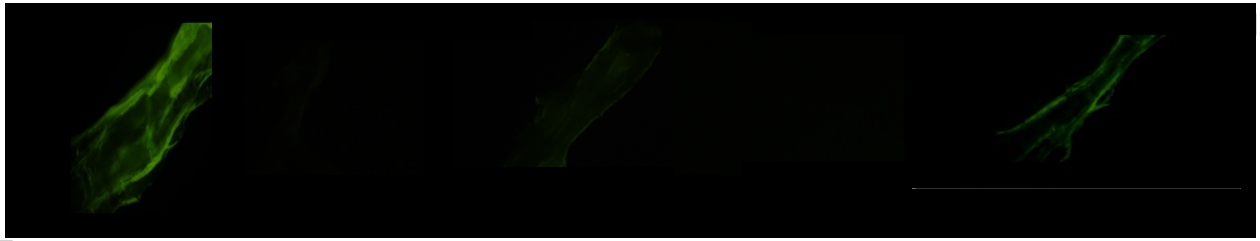

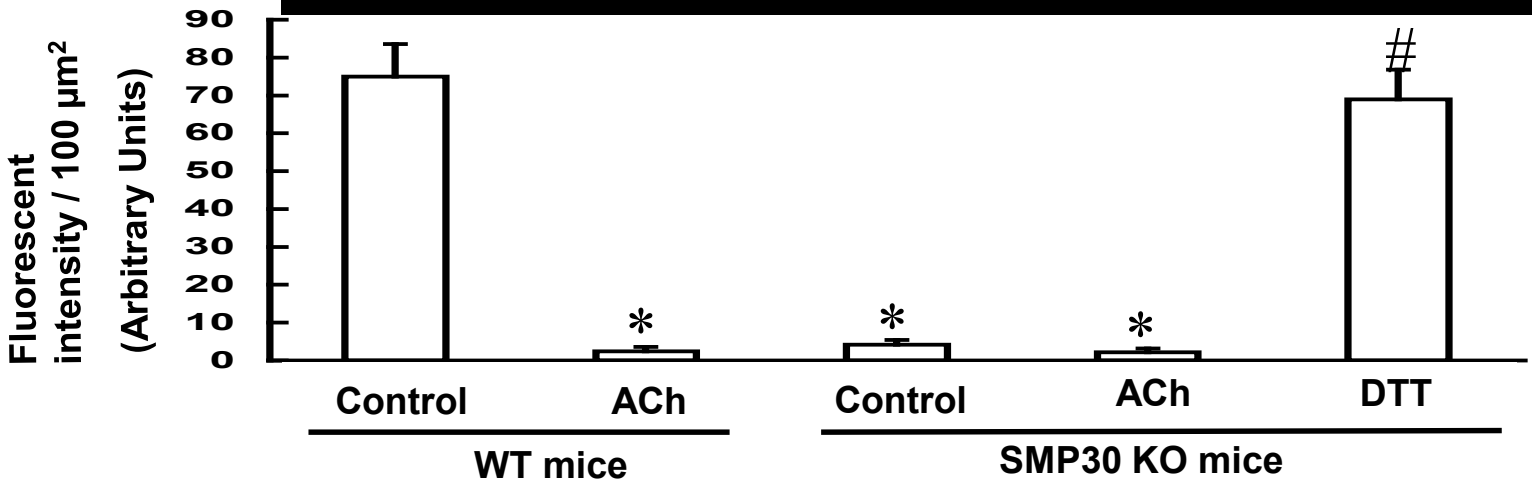
Fluorescent intensity / 100 μm² (Arbitrary Units)
90
80
70
60
50
40
30
20
10
0
*
*
*
#
Control
ACh
Control
ACh
DTT
WT mice
SMP30 KO mice

B

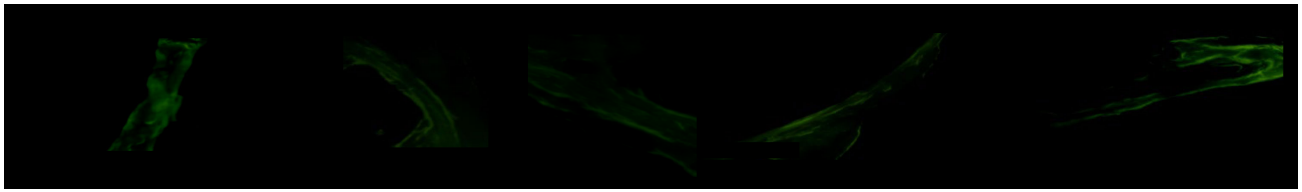

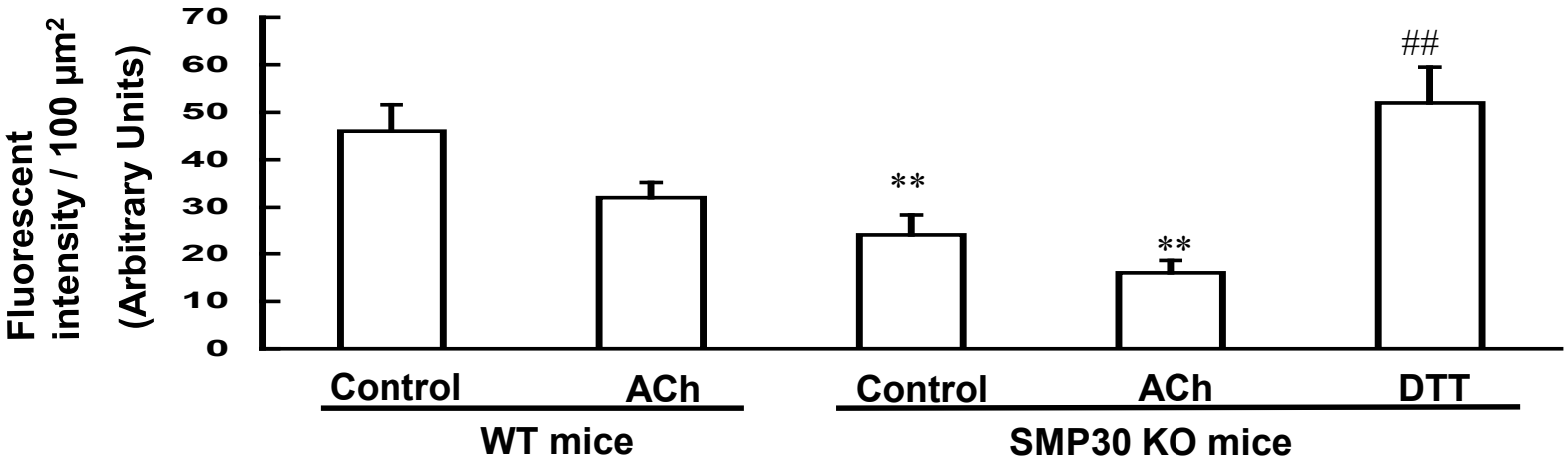
Fluorescent intensity / 100 μm² (Arbitrary Units)
70
60
50
40
30
20
10
0
**
**
##
Control
ACh
Control
ACh
DTT
WT mice
SMP30 KO mice

FIG. 9.

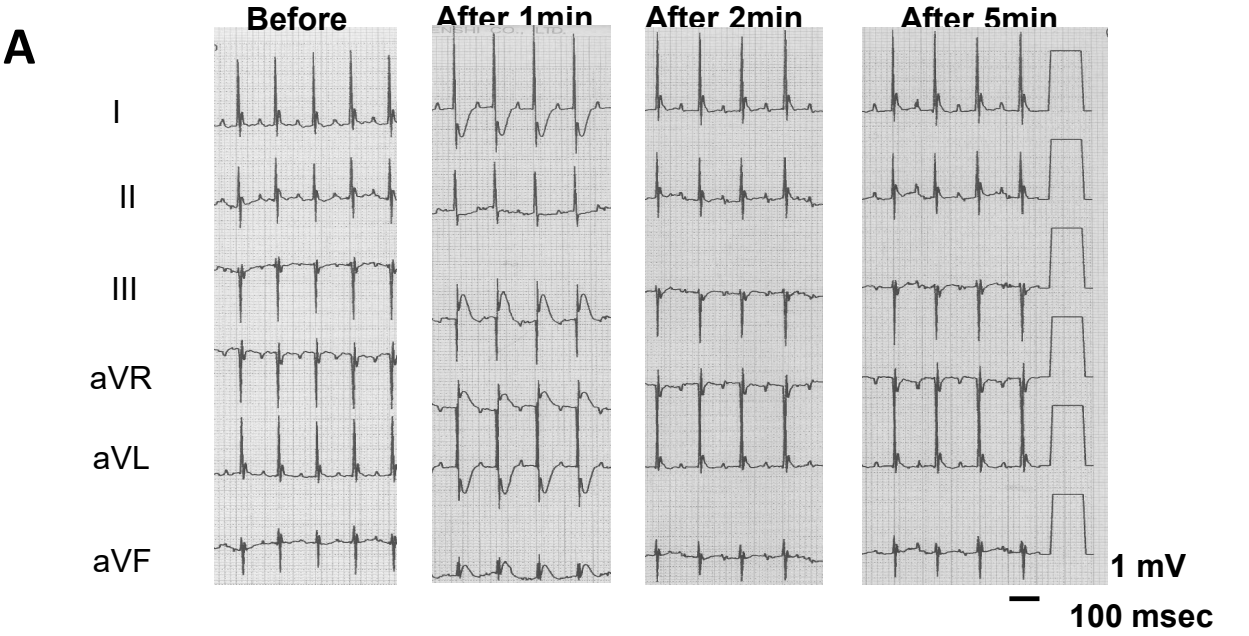
A
Before
After 1min
After 2min
After 5min
I
II
III
aVR
aVL
aVF
1 mV
100 msec
B
Before
After 1min
After 2min
After 5min
I
II
III
aVR
aVL
aVF
1 mV
100 msec

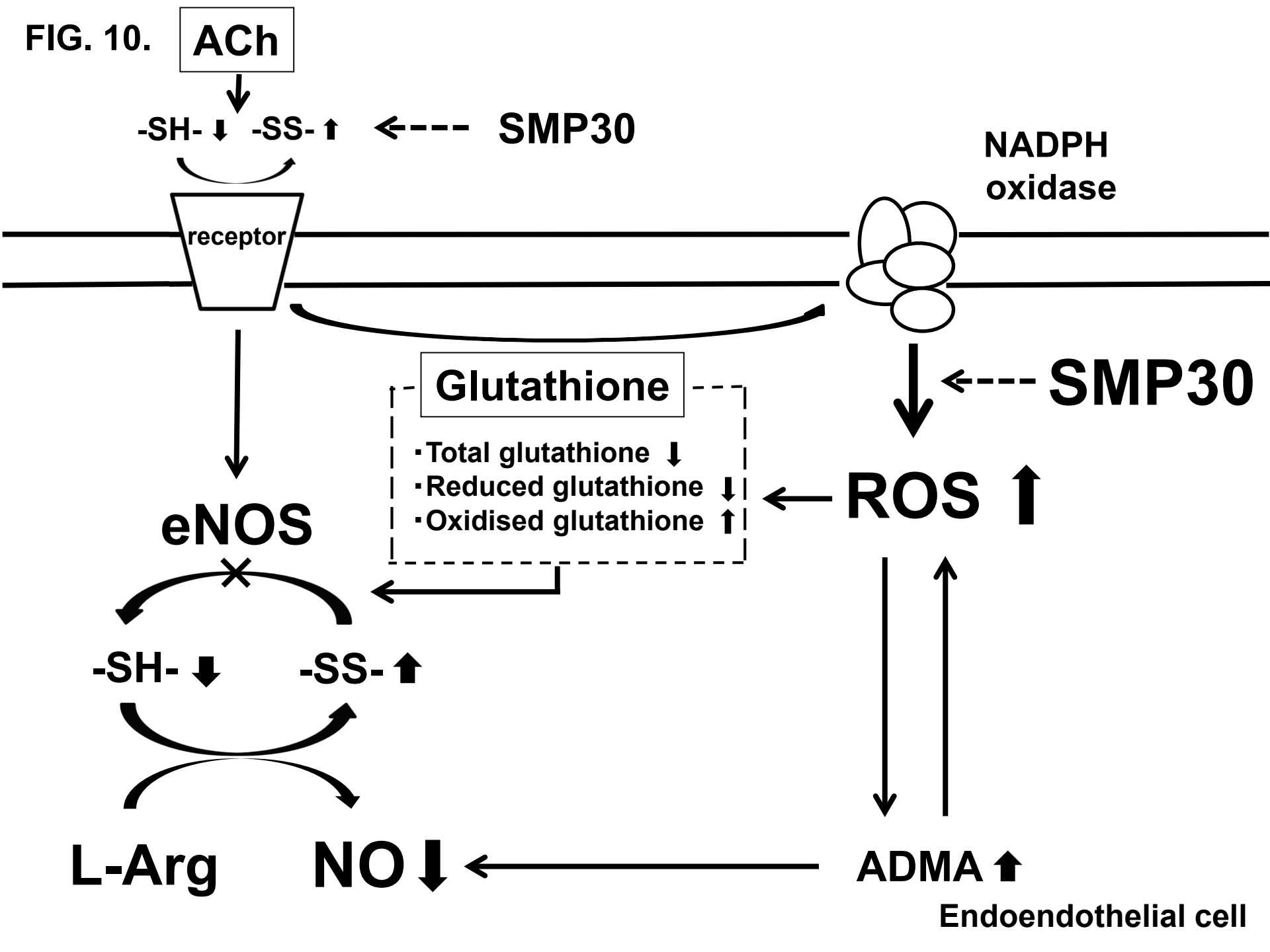
FIG. 10.
ACh
-SH- ⬇ -SS- ⬆
SMP30
NADPH oxidase
receptor
Glutathione
・Total glutathione ⬇
・Reduced glutathione ⬇
・Oxidised glutathione ⬆
SMP30
ROS ⬆
eNOS
-SH- ⬇
-SS- ⬆
L-Arg
NO ⬇
ADMA ⬆
Endoendothelial cell